



Carbon nanotube-enhanced electrochemical aptasensor for the detection of thrombin

Xiaorong Liu^a, Yan Li^{a,*}, Jianbin Zheng^{a,*}, Juncai Zhang^{a,b}, Qinglin Sheng^a

^a Institute of Analytical Science, Northwest University, Shaanxi Provincial Key Laboratory of Electroanalytical Chemistry, Xi'an, Shaanxi 710069, China

^b Department of Chemistry, Xianyang Normal University, Xianyang, Shaanxi 712000, China

ARTICLE INFO

Article history:

Received 19 November 2009
Received in revised form 3 March 2010
Accepted 9 March 2010
Available online 19 March 2010

Keywords:

Biosensor
Aptasensor
Carbon nanotubes
Aptamer
Thrombin

ABSTRACT

A novel electrochemical aptasensor for the detection of thrombin was developed on basis of the thrombin-binding aptamer (TBA) as a molecular recognition element and multi-walled carbon nanotubes (MWCNTs) as a carrier of the electrochemical capture probe. Amine-modified capture probe (12-mer) was covalently conjugated to the MWCNTs modified glassy carbon electrode (GCE). The target aptamer probe (21-mer) contains TBA (15-mer) labeled with ferrocene (Fc), which is designed to hybridize with capture probe and specifically recognize thrombin, is immobilized on the electrode surface by hybridization reaction. Introduction of the analyte thrombin triggered the dissociation of the aptamer probe labeled with Fc from the biosensors, led to a significant decrease in peak current intensity. Differential pulse voltammetry (DPV) was employed to detect the target analyte with different concentrations. The decreased peak current was in proportion to the concentration of thrombin in a range from 1.0×10^{-12} to 5.0×10^{-10} M with a detection limit of 5×10^{-13} M. The present work demonstrates that using MWCNTs as a carrier for electrochemical capture probe is a promising way to amplify the electrochemical signal and to improve the sensitivity of the electrochemical aptasensor.

© 2010 Elsevier B.V. All rights reserved.

1. Introduction

The detection and quantification of proteins play an essential role in fundamental research and clinical applications. Biosensors, which combine the perfect sensitivity and specificity of biologically active molecules with the suitable transducers, are simple, inexpensive analytical devices that provide escalating quantities of proteins information [1]. Many antibody-based biosensors can successfully detect and determine proteins. However, the utilization of antibodies may encounter some drawbacks with their production, stability, and modification, and searching for other alternative candidates is ongoing [2]. Aptamers are short single-stranded oligonucleotides selected for their high affinity and binding specifically to proteins or other targets [3]. Aptamers as molecular recognition substances for proteins appear to be excellent alternatives to antibodies due to their ease of production in vitro, wide target range, modification ease, reversible thermal denaturation, and unlimited shelf life [4]. Various aptasensor for proteins have been developed based on different technologies, such as quartz crystal microbalance [5], surface plasma resonance (SPR) [6], fluorescence [7–9], electrochemistry [10–12], electrogener-

ated chemiluminescence (ECL) [13,14], and colorimetry [15,16]. Among them, the electrochemical methods have attracted substantial attention in the development of aptasensors because of their high sensitivity, simple instrumentation, low production cost, fast response, portability, and inexpensiveness.

Extensive efforts have been devoted to developing some novel electrochemical aptasensors for the detection of proteins with high sensitivity. These efforts include the synthesis of new high-affinity aptamers and redox labels [17], the employment of highly sensitive detection techniques [18], the development of new electrode materials including nanomaterials [19,20] and the exploration of appropriate design strategies. The detection limits of these mentioned above electrochemical aptasensors are commonly in the nanomolar (nM) range. Many of protein biomarkers present at an ultralow level in the early stage of diseases. Therefore, developing ultrasensitive protein detection methods become a greater challenge. In order to amplify signals in protein detection, many methods have been introduced such as rolling circle amplification (RCA) [21,22], strand displacement amplification (SDA) [23,24] and enzyme label [25,26]. These methods bear the advantage of high sensitivity, yet suffers the disadvantages of their complexity, expensiveness and requirement of strict detection conditions as well.

Nanomaterials offer excellent prospects for chemical and biological sensing because of their unique electrical properties [27].

* Corresponding authors. Tel.: +86 29 88302077; fax: +86 29 88303448.
E-mail address: yanli@nwu.edu.cn (Y. Li).

In recent years, nanomaterials have been applied for the detection of DNA [28] and protein [29,30] with sensitivities in the pico- and femtomolar range. Several efforts have been devoted to developing a novel electrochemical aptasensor for the detection of proteins incorporating nanomaterials. Willner and co-workers [31] reported a thrombin sensor by employing aptamer-functionalized platinum nanoparticles as catalytic labels for the amplified electrochemical detection. Fang and co-workers [32] reported an ultrasensitive electrochemical sensor for detecting thrombin based on network-like thiocyanuric acid/gold nanoparticles. Wang and co-workers [33] reported aptamer/quantum-dot-based dual-analyte biosensor for the detection of thrombin and lysozyme. New nanomaterial-based schemes coupling of multiple amplification units and processes on surface are highly desired for meeting the high sensitivity of electrochemical aptasensor for the detection of protein. Carbon nanotubes (CNT) have been proved to be a novel type of nanostructure materials with attractive properties including unique mechanical, electronic and chemical properties [34]. The attractive properties of CNT make them promising candidates for aptasensor detection of protein [35–37]. Carbon nanotubes used in the electrochemical aptasensors, and as an immobilized carrier, dramatically increases the surface loading of capture probe and amplifies the electrochemical signal.

The aim of the present work is to develop nanomaterial amplified sensitive electrochemical protein aptasensor. In present work, thrombin was chosen as a model of target analyte and TBA was taken as a molecular recognition element. MWCNTs were employed as the carriers of the electrochemical capture probe to amplify the change of peak current upon combining of thrombin. An electrochemical aptasensor was designed and the electrochemical characteristics of an electrochemical aptasensor fabricated were investigated. To our knowledge, this is the new example of electrochemical aptasensor for the detection of thrombin using MWCNTs as a carrier of the electrochemical capture probe.

2. Experimental

2.1. Chemicals and reagents

Multi-walled carbon nanotubes (MWCNTs) were purchased from Shenzhen Nanotech Port Co. Ltd. (Shenzhen, China). Human α -thrombin ($M_w = 36, 7000$ kDa, $pI = 7.0$ – 7.6) was purchased from Haematologic (USA). Ferrocene carboxylic acid (Fc), 1-ethyl-3-(3-dimethylaminopropyl) carbodiimide (EDC), *N*-hydroxysuccinimide (NHS), bovine serum albumin (BSA) and bovine hemoglobin (Hb) were purchased from Sigma (USA). All reagents were analytical grade. Millipore Milli-Q water (18 M Ω cm) was used throughout. 0.10 M phosphate buffer solution (PBS, pH 7.0) was used as hybridization, binding and washing solution. Aptamers were synthesized by Shenggong Bioengineering Ltd. Company (Shanghai). A 21-mer target aptamer probe (Tgt-aptamer) adopted from literature [38] was used to bind with thrombin: 5'-CAC TGT GGT TGG TGT GGT TGG-(CH₂)₆-NH₂-3'. A shorter (12-mer) partial complementary DNA of Tgt-aptamer was covalently conjugated to the MWCNTs modified glassy carbon electrode as the "capture" DNA (Cpt-DNA) to hold the Tgt-aptamer: 5'-CCA ACC ACA GTG-(CH₂)₆-NH₂-3'.

2.2. Apparatus

Cyclic voltammetry (CV), differential pulse voltammetry (DPV) and electrochemical impedance spectroscopy (EIS) measurements were performed with CHI 660a electrochemical workstation (Shanghai Chenhua Instrument Corporation, China). All experiments were carried out using a conventional three-electrode

system with a fabricated aptasensor with a GCE ($\phi = 2.0$ mm) as the working electrode, a platinum wire as the counter electrode and a saturated calomel reference electrode (SCE). All potentials were referred to this reference electrode. Scanning electron microscopic (SEM) images were acquired with a JSM-6380 scanning electron microscope (JEOL Ltd., Japan).

2.3. Preparation of MWCNTs-COOH

The carboxyl functionalized MWCNTs were prepared as reported in the literature [39,40]. Briefly, 100 mg MWCNTs were dispersed in 100 mL of a nitric acid and sulfuric acid (1:3) mixture solution. The mixture solution was ultrasonically agitated for 30 min and then refluxed for 4 h at 80 °C. After that, the MWCNTs were filtered and rinsed with distilled water until the filtrate became neutral. Then the precipitate was dried under an infrared lamp. That was, the MWCNTs-COOH. The MWCNTs-COOH suspension was prepared by dispersing 2 mg MWCNTs-COOH in 10 mL of organic solvent *N,N*-dimethylformamide (DMF) with the aid of ultrasonic agitation [41,42]. The prepared MWCNTs-COOH was characterized with SEM.

2.4. Synthesis of Fc-labeled thrombin aptamer

The ferrocene label was conjugated to the 3'-amine-modified Tgt-aptamer (abbreviated as Fc-Tgt-aptamer) by the succinimide coupling (EDC-NHS) [43]. Briefly, 100 μ L of 10 μ M Tgt-aptamer and 100 μ L of 10 mM PBS (pH 7.0) containing 10 mM ferrocenecarboxylic acid, 1 mM EDC, and 5 mM NHS were together and then incubated at 37 °C for 2 h. The conjugate was dialyzed against 10 mM PBS (500 mL) for 12 h to remove excessive ferrocenecarboxylic acid. Finally, the mixture was stored in the refrigerator at -20 °C. Note that degraded or unlabeled DNA after the conjugation reaction only caused a slight loss of the sensitivity but had no effect on the specificity of the biosensor.

2.5. Fabrication of electrochemical aptasensors of thrombin

The GCE was pretreated as previously described [44]. The aptasensor was fabricated as follows: 10 μ L of 2 mg mL⁻¹ suspension of MWCNTs-COOH was dropped onto a freshly smoothed GCE surface uniformly, and the solvent was then evaporated under an infrared lamp. The electrode was thoroughly rinsed, the first with ethanol, and then with ultrapure water to remove excessive nanotubes. The MWCNTs-COOH modified GCE was immersed in 1 mL PBS containing 10 mM NHS and 10 mM EDC in order to activate the carboxyl of MWCNTs-COOH. After 1 h, the modified electrode was rinsed again and transferred in 500 μ L of 3.5×10^{-6} M Cpt-DNA for 2 h. The Cpt-DNA modified electrode was immersed in 100 μ L of 1.0×10^{-6} M Fc-Tgt-aptamer for 1 h to form the sensing interface in 0.10 M PBS. The resulting electrode was used as an aptasensor of thrombin.

2.6. Electrochemical measurement

The aptasensor fabricated was immersed in 100 μ L of 0.10 M PBS containing different concentrations of thrombin for 30 min at 37 °C, followed by thoroughly washing with 0.10 M PBS to remove unbound thrombin. The electrode was transferred into electrochemical cell. The DPV measurement was performed in the potential range from 0.2 to 0.6 V with pulse amplitude of 50 mV. The concentration of thrombin was quantified by the oxidation peak current at +0.364 V.

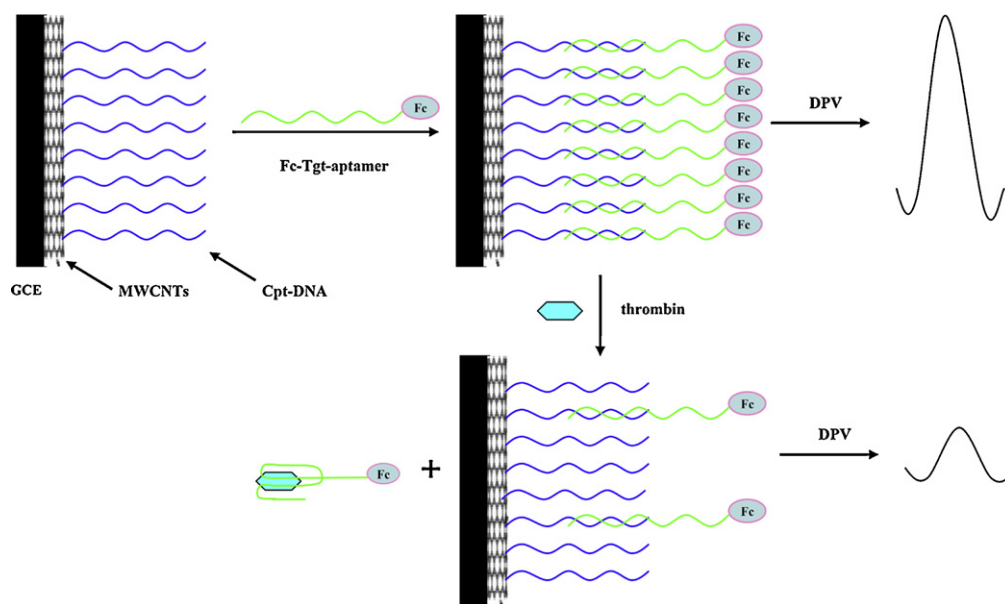


Fig. 1. Scheme diagram of the carbon nanotube-enhanced electrochemical aptasensor for the detection of thrombin.

3. Results and discussion

3.1. Design and characterization of aptasensor

Schematic diagram of the electrochemical aptasensor for the detection of thrombin is demonstrated in Fig. 1. An intact aptamer labeled with Fc was used as the detection probe (Fc-Tgt-aptamer). The Fc-Tgt-aptamer comprises three segments: the first segment (in blue) is a six-base segment close to the 5'-terminal that could hybridize with Cpt-DNA close to the 3'-terminal; the second segment (in green) is the aptamer sequence for thrombin, whose six-base segment could hybridize with the 5'-terminal six-base segment of Cpt-DNA; the third segment is a Fc label, which is coupled at 3'-terminus and employed as the electrochemical signal producer. When the biosensor was immersed into an analyte solution, the interaction between thrombin and Fc-Tgt-aptamer resulted in the displacement of Fc-Tgt-aptamer from the electrode surface while Cpt-DNA was still bound to electrode surface. DNA secondary structures are less stable than G-quadruplex aptamer because of weaker stacking energies [45,46]. It is well documented that aptamers have typical affinities (K_d) in the nM range (or lower) for protein targets. An aptamer can bind tightly and specifically to a variety of proteins to form an aptamer-protein complex with a binding constant greater than that of an ordinary DNA duplex [47]. Therefore, in the absence of thrombin, the Fc-Tgt-aptamer would bind to the surface immobilized Cpt-DNA. Then a strong current signal would be observed when an appropriate potential was applied. However, in the presence of thrombin, the Tgt-aptamer preferred to form a Tgt-aptamer-thrombin complex, which was thermodynamically more stable [48]. As a result, the Fc-Tgt-aptamer would leave from the electrode surface with thrombin and result in decreased current.

CV and EIS were used for monitoring the process of the fabrication of electrochemical aptasensor in each step. As can be seen from Fig. 2, the MWCNTs-COOH/GCE (Fig. 2, curve b) had larger CV current than bare GCE (Fig. 2, curve a), which ascribed to the fact that modification of the electrode with MWCNTs-COOH could significantly enhance the effective electrode surface area as well as provide an active binding group for oligonucleotides derivation. A current decrease (Fig. 2, curve c) appeared after exposing to Cpt-DNA. It is well-known that a covalently conjugated Cpt-DNA as an electron-transfer blocking layer can hinder

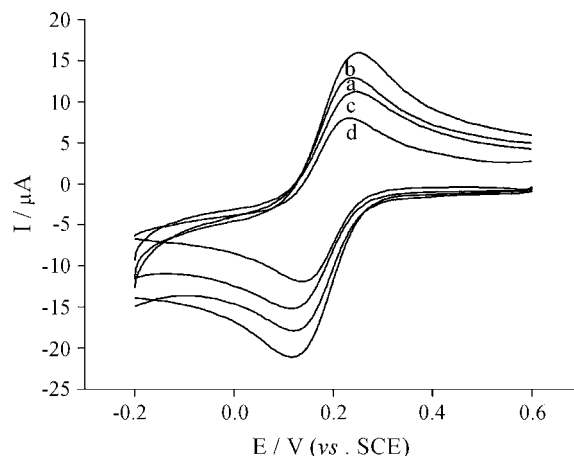


Fig. 2. CV obtained in 0.10 M PBS containing 1 mM $\text{Fe}(\text{CN})_6^{3-}/\text{Fe}(\text{CN})_6^{4-}$ and 0.1 M KCl at a scan rate of 50 mV s^{-1} at a bare GCE (a), MWCNTs-COOH/GCE (b), Cpt-DNA/MWCNTs-COOH/GCE (c), Fc-Tgt-aptamer/Cpt-DNA/MWCNTs-COOH/GCE (d).

the diffusion of ferricyanide toward the electrode surface [49]. The hybridization of Fc-Tgt-aptamer with Cpt-DNA on the electrode surface led to the further decrease of electron-transfer efficiency (Fig. 2, curve d) due to the introduction of additional negative surface charges. These results demonstrated that aptamer probe was successfully fixed on the electrode and a sensing interface was obtained. Ferrocene and potassium ferrocyanide present similar oxidation responses. The 1 mM potassium ferrocyanide exhibits a substantially larger current signal for the significantly (1000-fold) lower Fc-Tgt-aptamer concentration. The oxidation peak of potassium ferrocyanide was overlapping with the oxidation peak of Fc in the Fig. 2. The interference between ferrocene and potassium ferrocyanide could be neglected in the experiments performed with potassium ferro/ferricyanide (CV).

Fig. 3 showed Nyquist plots of impedance spectra obtained at different electrodes. The change in semicircle diameter is a result in the change in the interfacial resistance R_{et} to electron transfer from their modified electrode to ferricyanide in solution. From Fig. 3, it can be seen that the bare GCE exhibits a very small semicircle domain, suggesting a very low electron-transfer resistance

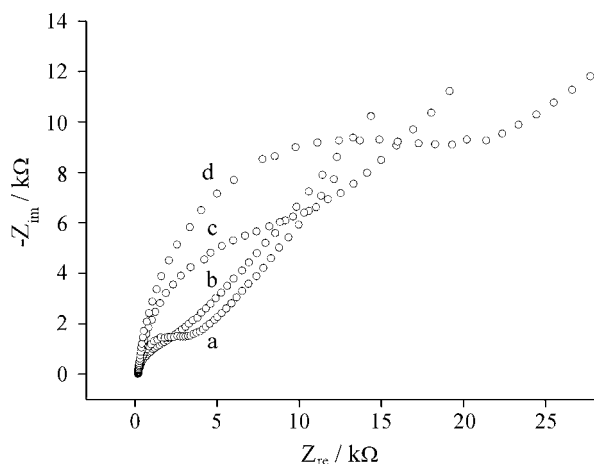


Fig. 3. Nyquist plots of impedance spectra obtained in 0.10 M PBS containing 1 mM $\text{Fe}(\text{CN})_6^{3-}/\text{Fe}(\text{CN})_6^{4-}$ and 0.1 M KCl at a bare GCE (a), MWCNTs-COOH/GCE (b), Cpt-DNA/MWCNTs-COOH/GCE (c), Fc-Tgt-aptamer/Cpt-DNA/MWCNTs-COOH/GCE (d). The biased potential was 0.172 V. The frequency was from 100 kHz to 0.1 Hz and the amplitude was 5.0 mV.

to the redox probe dissolved in the electrolyte solution (Fig. 3, curve a). The electrochemical response was a nearly straight line (Fig. 3, curve b), which indicates that MWCNTs are modified onto the surface of GCE. After Cpt-DNA was covalently conjugated onto the surface of MWCNTs-COOH/GCE, the R_{et} markedly increased to 6489 Ω (Fig. 3, curve c). This is attributed to the fact that the redox couple of $\text{K}_3[\text{Fe}(\text{CN})_6]/\text{K}_4[\text{Fe}(\text{CN})_6]$ is suffered electrostatic repulsive forces from the covalently conjugated Cpt-DNA [50]. Hybridizing with the Fc-Tgt-aptamer, the impedance value further increased to 13890 Ω (Fig. 3, curve d). The changes of R_{et} for the different steps were in agreement with the results as seen in the CV, which further confirmed the successful immobilization of Cpt-DNA on the MWCNTs-COOH/GCE surface, the hybridization between the Cpt-DNA and Fc-Tgt-aptamer.

Fig. 4 shows the DPV of the electrochemical aptasensors fabricated before (Fig. 4, curve a) and after interaction with 5.0×10^{-11} M thrombin (Fig. 4, curve b) and 1.0×10^{-10} M thrombin (Fig. 4, curve c), respectively. Compared curve a with curve b, electrochemical aptasensors with interaction of 5.0×10^{-11} M thrombin displayed a lower peak current. This indicates that the

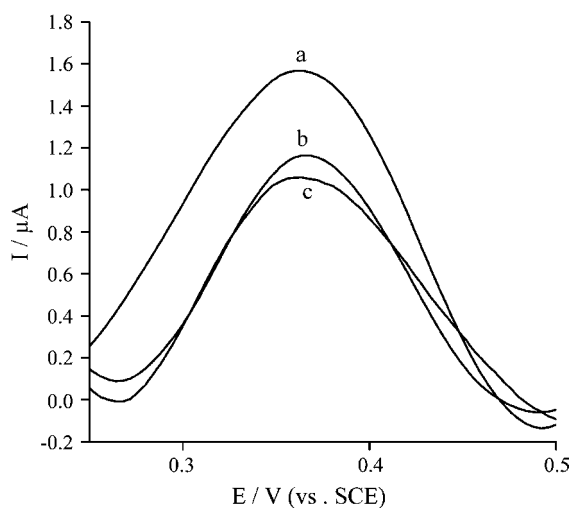


Fig. 4. DPVs of the aptasensor in 0.10 M PBS in the absence of thrombin (a) and in the presence of 5.0×10^{-11} M (b) and 1.0×10^{-10} M (c) thrombin at a scan rate of 50 mV s^{-1} . DPV parameters: pulse amplitude 50 mV, pulse width 50 ms, pulse period 0.2 s.

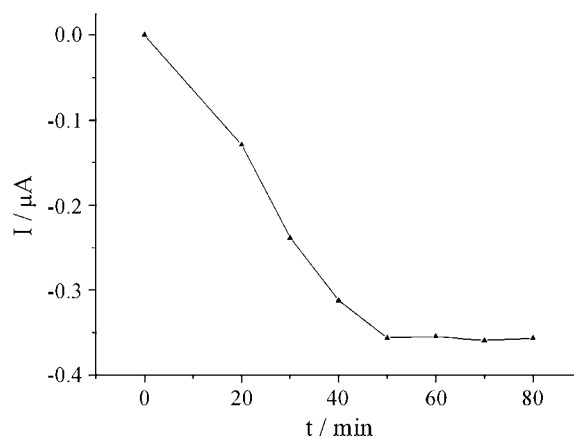


Fig. 5. Effect of hybridization time between Cpt-DNA and Fc-Tgt-aptamer on the current response of the aptasensor to 1.0×10^{-11} M thrombin in 0.10 M PBS. Other conditions are the same as in Fig. 4.

aptasensor can response to analyte thrombin. Compared curve b with curve c, it can be clearly observed that the peak current decreases from 1.139 μA to 1.02 μA as the thrombin concentration is elevated. This indicates that the peak current decreased is consistent with the increasing the concentration of thrombin. Therefore, the electrochemical aptasensors possibly can be used to detect of target thrombin.

3.2. Optimization of hybridization time and incubation time

Important experimental parameters including hybridization time and incubation time were optimized to obtain a high sensitivity of the fabricated electrochemical aptasensor. The hybridization time between Cpt-DNA and Fc-Tgt-aptamer was investigated as it can influence the hybridization efficiency and the succeeding response to thrombin. The effect of the hybridization time on the increased peak current at 1.0×10^{-11} M thrombin was investigated. Fig. 5 shows the effect of hybridization time on the peak current intensity. The results showed that the decrement of peak current (ΔI_{peak}) increased with increasing the hybridization time and reached equilibrium more than 50 min. To ensure the completeness of hybridization between Cpt-DNA sequences and Fc-Tgt-aptamer 60 min was set as the hybridization time in whole experiments. Beside the effect of hybridization time, it was found that a different incubation time of thrombin caused a visible difference in the decrease of peak current. Therefore, the dependence of thrombin incubation time on the decrease of the peak current was studied to determine the optimum incubation time of thrombin. As shown in Fig. 6, the peak current decreased immediately when 1.0×10^{-11} M thrombin was introduced and then tended to stabilize after more than 25 min. Considering the fact that the specific interaction of aptamer with thrombin at a lower concentration needs longer time, 30 min was chosen as the thrombin incubation time.

3.3. Performance of the aptasensor

3.3.1. Linear range and detection limit

The introduction of thrombin at different concentrations to the aptasensor induced different decreases in peak current associated with the amount of the released Fc-Tgt-aptamer. Series samples of 1.0×10^{-12} to 1.0×10^{-7} M thrombin were determined by the aptasensor. Fig. 7 shows the DPV profiles of the aptasensor after interaction with different concentrations of thrombin under the optimized conditions. From Fig. 7, it can be seen that the peak current decreases with an increase of the concentration of thrombin. The peak current was logarithmically related to concentration of

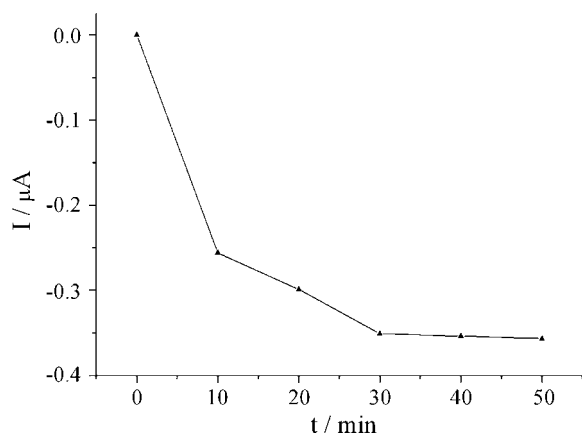


Fig. 6. Effect of thrombin incubation time on the current response of the aptasensor to 1.0×10^{-11} M thrombin in 0.10 M PBS. Other conditions are the same as in Fig. 4.

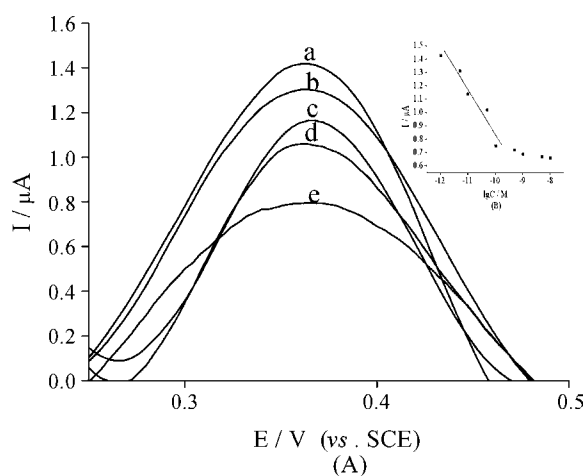


Fig. 7. (A) DPVs of the aptasensor for the detection of different concentrations of thrombin (a) 1.0×10^{-12} M, (b) 1.0×10^{-11} M, (c) 5.0×10^{-11} M, (d) 1.0×10^{-10} M, (e) 5.0×10^{-10} M. (B) The linear relationship between the peak current and the concentration of thrombin. The DPV conditions are same as Fig. 4.

thrombin in the range from 1.0×10^{-12} to 5.0×10^{-10} M. The calibration equation was $I = 0.960 - 0.210 \lg C$ (unit of C is μM) and the correlation coefficient was 0.9984 (shown in the inset of Fig. 7). The detection limit was 5×10^{-13} M based on a signal-to-noise ratio of 3. This demonstrates that the MWCNTs as electrochemical capture probe carriers amplification are effective for the enhancement of the sensitivity of the aptasensor, which would provide a promising foundation for the signal amplification in the field of bioassay. Meanwhile, the detection limit obtained using the present sensing system is 5000-fold lower than the literature value achieved using an electrochemical method coupled to gold nanoparticle [2]. And ~ 2 orders of magnitude lower than the detection limit reported impedimetric aptasensor [51].

3.3.2. Selectivity

BSA and Hb, which belong to the proteins family, were examined for their interference effect. Fig. 8 exhibited different peak current signals of the proposed sensing system after the addition of 5.0×10^{-10} M thrombin, 5.0×10^{-10} M BSA or 5.0×10^{-10} M Hb under the same experimental conditions. Only the thrombin sample gave significant decreased peak current, while the same concentration of two proteins had slight emissions which were equivalent to that of the blank measurement. These tests indicated that the developed strategy could be used to identify thrombin with high specificity.

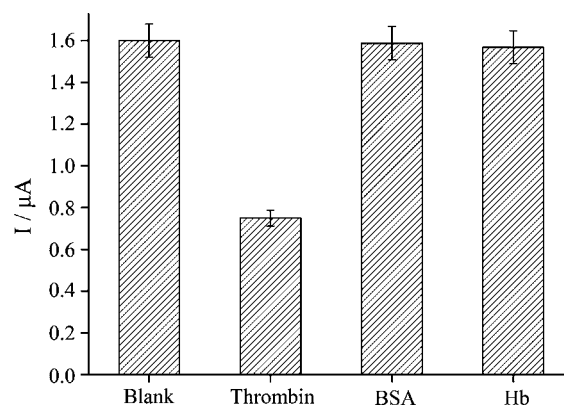


Fig. 8. Specificity of the aptasensor to 5.0×10^{-10} M thrombin by comparing it to the interfering agents, including two proteins at the same concentration: BSA, Hb. The DPV conditions are same as Fig. 4.

4. Conclusions

A novel electrochemical aptasensor for the detection of thrombin was developed on basis of the thrombin-binding aptamer taken as a molecular recognition element, Fc as a redox tag of Tgt-aptamer and MWCNTs as a carrier of the electrochemical capture probe. The developed aptasensor exhibited high sensitivity and selectivity. This work demonstrates that MWCNTs modified GCE can provide a promising platform for electrochemical capture probe immobilization and greatly enhance the sensitivity of electrochemical aptasensor due largely to the specific area of the MWCNTs which provide high capturing for molecular recognition elements. The proposed biosensor provides a promising strategy for the detection of other proteins.

Acknowledgements

Financial supports from the National Science Foundations of China (No. 20875076), the Specialized Research Fund for the Doctoral Program of Higher Education of China (No. 20096101120011), the Education Department of Shaanxi Province, China (No. 09JK759) and the NWU Graduate Innovation and Creativity Funds (No. 09YSY04) are gratefully acknowledged.

References

- [1] A.P.F. Turner, Science 290 (2000) 1315.
- [2] H. Xu, X. Mao, Q. Zeng, S. Wang, A.-N. Kawde, G. Liu, Anal. Chem. 81 (2009) 669.
- [3] D. Shanguan, Y. Li, Z. Tang, Z. Cao, H. Chen, P. Mallikaratchy, K. Sefah, C. Yang, W. Tan, Proc. Natl. Acad. Sci. USA 103 (2006) 11838.
- [4] M. Famulok, J.S. Hartig, G. Mayer, Chem. Rev. 107 (2007) 3715.
- [5] L. Michael, B. Petersen, H. Wolf, E. Prohaska, Anal. Chem. 74 (2002) 4488.
- [6] S.J. Lee, B.S. Youn, J.W. Park, J.H. Niaz, Y.S. Kim, M.B. Gu, Anal. Chem. 80 (2008) 2867.
- [7] V. Pavlov, B. Shlyahovsky, I. Willner, J. Am. Chem. Soc. 127 (2005) 6522.
- [8] Y. Jiang, X. Fang, C. Bai, Anal. Chem. 76 (2004) 5230.
- [9] R. Nutiu, Y. Li, Angew. Chem. Int. Ed. 44 (2005) 1061.
- [10] R. Polsky, R. Gill, I. Willner, Anal. Chem. 78 (2006) 2268.
- [11] Y. Xiao, B.D. Piorek, K.W. Plaxco, A.J. Heeger, J. Am. Chem. Soc. 127 (2005) 17990.
- [12] Y.G. Peng, D.D. Zhang, Y. Li, H.L. Qi, Q. Gao, C.X. Zhang, Biosens. Bioelectron. 25 (2009) 94.
- [13] Y. Li, H.L. Qi, Y.G. Peng, J. Yang, C.X. Zhang, Electrochem. Commun. 10 (2007) 2571.
- [14] Y. Li, H.L. Qi, Y.G. Peng, Q. Gao, C.X. Zhang, Electrochem. Commun. 10 (2008) 1322.
- [15] C.C. Huang, Y.F. Huang, Z. Cao, W. Tan, H.T. Chang, Anal. Chem. 77 (2005) 5735.
- [16] J.W. Liu, Y. Lu, Angew. Chem. Int. Ed. 45 (2006) 90.
- [17] J.A. Hansen, J. Wang, A.N. Kawde, Y. Xiang, K.V. Gothelf, G. Collins, J. Am. Chem. Soc. 128 (2006) 2228.
- [18] R.Y. Lai, K.W. Plaxco, A.J. Heeger, Anal. Chem. 79 (2007) 229.
- [19] Y. Du, B.L. Li, H. Wei, Y.L. Wang, E.K. Wang, Anal. Chem. 80 (2008) 5110.
- [20] J.G. Bai, H. Wei, B.L. Li, L.H. Song, L.Y. Fang, Z.Z. Lü, W.H. Zhou, E.K. Wang, Chem. Asian J. 3 (2008) 1935.

- [21] L. Zhou, L.J. Ou, X. Chu, G.L. Shen, R.Q. Yu, *Anal. Chem.* 79 (2007) 7492.
- [22] L. Yang, C.W. Fung, E.J. Cho, A.D. Ellington, *Anal. Chem.* 79 (2007) 3320.
- [23] B. Shlyahovsky, D. Li, Y. Weixmann, R. Nowarski, M. Kotler, I. Willner, *J. Am. Chem. Soc.* 129 (2007) 3814.
- [24] Y. Weizmann, M.K. Beissenhirtz, Z. Cheglakov, R. Nowarski, M. Kotler, I. Winler, *Angew. Chem. Int. Ed.* 45 (2006) 7384.
- [25] F. Patolsky, E. Katz, I. Willner, *Angew. Chem. Int. Ed.* 41 (2002) 3398.
- [26] L. Alfonta, A. Bardea, O. Khersonsky, E. Katz, I. Willner, *Biosens. Bioelectron.* 16 (2001) 675.
- [27] P. Bertocello, R.J. Forster, *Biosens. Bioelectron.* 24 (2009) 3191.
- [28] J.A. Hansen, R. Mukhopadhyay, J.O. Hansen, K.V. Gothelf, *J. Am. Chem. Soc.* 128 (2006) 3860.
- [29] G. Jie, B. Liu, H. Pan, J.J. Zhu, H.Y. Chen, *Anal. Chem.* 79 (2007) 5574.
- [30] X. Yu, B. Munge, V. Patel, G. Jensen, A. Bhirde, J.D. Gong, S.N. Kim, J. Gillespie, J.S. Gutkind, F. Papadimitrakopoulos, J.F. Rusling, *J. Am. Chem. Soc.* 128 (2006) 11199.
- [31] R. Polsky, R. Gill, L. Kaganovsky, I. Willner, *Anal. Chem.* 78 (2006) 2268.
- [32] J. Zheng, W.J. Feng, L. Lin, F. Zhang, G.F. Cheng, P.G. He, Y.Z. Fang, *Biosens. Bioelectron.* 23 (2007) 341.
- [33] J.A. Hansen, J. Wang, A.-N. Kawde, Y. Xiang, K.V. Gothelf, G. Collins, *J. Am. Chem. Soc.* 128 (2006) 2228.
- [34] D. Tasis, N. Tagmatarchis, A. Bianco, M. Prato, *Chem. Rev.* 106 (2006) 1105.
- [35] H.-M. So, K.Y.H. Won, B.-K. Kim, B.H. Ryu, P.S. Na, H. Kim, J.-O. Lee, *J. Am. Chem. Soc.* 127 (2005) 11906.
- [36] R. Yang, Z. Tang, J. Yan, H. Kang, Y. Kim, Z. Zhu, W. Tan, *Anal. Chem.* 80 (2008) 7408.
- [37] G. Evtugyn, A. Porfireva, M. Ryabova, T. Hianik, *Electroanalysis* 20 (2008) 2301.
- [38] Z.S. Wu, M.M. Guo, S.B. Zhang, C.R. Chen, J.H. Jiang, G.L. Shen, R.Q. Yu, *Anal. Chem.* 79 (2007) 2933.
- [39] H. Cai, X. Cao, Y. Jiang, P.G. He, Y.Z. Fang, *Anal. Bioanal. Chem.* 375 (2003) 287.
- [40] Q.L. Sheng, J.B. Zheng, *Biosens. Bioelectron.* 6 (2009) 1621.
- [41] J. Wang, M. Li, Z. Shi, N. Li, Z. Gu, *Anal. Chem.* 74 (2002) 1993.
- [42] K.B. Male, S. Hrapovic, J.M. Santini, J.H.T. Luong, *Anal. Chem.* 79 (2007) 7831.
- [43] R.P. Fahlman, D. Sen, *J. Am. Chem. Soc.* 124 (2002) 4610.
- [44] S. Niu, M. Zhao, L. Hu, S.S. Zhang, *Sens. Actuators B: Chem.* 135 (2008) 200.
- [45] J.J. SantaLucia, *Proc. Natl. Acad. Sci. USA* 95 (1998) 1460.
- [46] L.S. Green, D. Jellinek, R. Jenison, A. Ostman, C.H. Heldin, N. Janjic, *Biochemistry* 35 (1996) 14413.
- [47] J.J. SantaLucia, D. Hicks, *Annu. Rev. Biophys. Biomol. Struct.* 33 (2004) 415.
- [48] T. Hermann, D.J. Patel, *Science* 287 (2002) 820.
- [49] M. Cho, S. Lee, S.-Y. Han, J.-Y. Park, M.A. Rahmen, Y.-B. Shim, C. Ban, *Nucleic Acids Res.* 34 (2006) 75.
- [50] A.E. Radi, J.L.A. Sanchez, E. Baldrich, C.K. O'Sullivan, *Anal. Chem.* 77 (2005) 6320.
- [51] Z. Zhang, W. Yang, J. Wang, C. Yang, F. Yang, X. Yang, *Talanta* 78 (2009) 1240.